Journal of Hazardous Materials 425 (2022) 127956

Contents lists available at ScienceDirect

Journal of Hazardous Materials

journal homepage: www.elsevier.com/locate/jhazmat

Research Paper

Foraging plasticity diversifies mercury exposure sources and bioaccumulation patterns in the world's largest predatory fish

Gaël Le Croizier [a,b,*], Jeroen E. Sonke [a], Anne Lorrain [c], Marina Renedo [a], Mauricio Hoyos-Padilla [d,e], Omar Santana-Morales [f], Lauren Meyer [g,h], Charlie Huveneers [g], Paul Butcher [i], Felipe Amezcua-Martinez [b], David Point [a]

[a] UMR Géosciences Environnement Toulouse (GET), Observatoire Midi Pyrénées (OMP), 14 avenue Edouard Belin, 31400 Toulouse, France
[b] Instituto de Ciencias del Mar y Limnología, Universidad Nacional Autónoma de México, Av. Joel Montes Camarena S/N, Mazatlán, Sin 82040, Mexico
[c] Univ Brest, CNRS, IRD, Ifremer, LEMAR, F-29280 Plouzané, France
[d] Pelagios-Kakunjá A.C, Sinaloa 1540, Col. Las Garzas, C.P. 23070 La Paz, B.C.S., Mexico
[e] Fins Attached: Marine Research and Conservation, 19675 Still Glen Drive, Colorado Springs, CO 80908, USA
[f] ECOCIMATI A.C., 22800 Ensenada, Baja California, Mexico
[g] Southern Shark Ecology Group, College of Science and Engineering, Flinders University, Adelaide, SA 5042, Australia
[h] Georgia Aquarium, Atlanta, GA 30313, USA
[i] NSW Department of Primary Industries, National Marine Science Centre, Coffs Harbour, NSW 2450, Australia

ARTICLE INFO

Editor: Dr. C. LingXin

ABSTRACT

Large marine predators exhibit high concentrations of mercury (Hg) as neurotoxic methylmercury, and the potential impacts of global change on Hg contamination in these species remain highly debated. Current contaminant model predictions do not account for intraspecific variability in Hg exposure and may fail to reflect the diversity of future Hg levels among conspecific populations or individuals, especially for top predators displaying a wide range of ecological traits. Here, we used Hg isotopic compositions to show that Hg exposure sources varied significantly between and within three populations of white sharks (*Carcharodon carcharias*) with contrasting ecology: the north-eastern Pacific, eastern Australasian, and south-western Australasian populations. Through Δ^{200}Hg signatures in shark tissues, we found that atmospheric Hg deposition pathways to the marine environment differed between coastal and offshore habitats. Discrepancies in δ^{202}Hg and Δ^{199}Hg signatures among white sharks provided evidence for intraspecific exposure to distinct sources of marine methylmercury, attributed to population and ontogenetic shifts in foraging habitat and prey composition. We finally observed a strong divergence in Hg accumulation rates between populations, leading to three times higher Hg concentrations in large Australasian sharks compared to north-eastern Pacific sharks, and likely due to different trophic strategies adopted by adult sharks across populations. This study illustrates the variety of Hg exposure sources and bioaccumulation patterns that can be found within a single species and suggests that intraspecific variability needs to be considered when assessing future trajectories of Hg levels in marine predators.

1. Introduction

The Anthropocene era has led to the global decline of shark populations, due to overfishing, bycatch, and other indirect threats including habitat loss and changes in prey availability (Baum et al., 2003; Myers and Worm, 2003; Ferretti et al., 2018; Dulvy et al., 2021). Removing predators can result in trophic cascading effects impairing the structure and functioning of marine ecosystems (Heithaus et al., 2008; Ferretti et al., 2010; Pimiento et al., 2020). In this context, it has recently been suggested that the white shark (*Carcharodon carcharias*), the world's largest predatory fish, may become extinct during the 21st century, along with its ecosystem role as apex predator (Pimiento et al., 2020). Despite a global decline in abundance over the past half century, the different populations of white sharks do not follow the same trajectories (Pacoureau et al., 2021). While some populations are considered stable, including in eastern Australasia (Davenport et al., 2021), a

* Corresponding author at: Instituto de Ciencias del Mar y Limnología, Universidad Nacional Autónoma de México, Av. Joel Montes Camarena S/N, Mazatlán, Sin 82040, Mexico.
E-mail address: gael.lecroizier@hotmail.fr (G. Le Croizier).

https://doi.org/10.1016/j.jhazmat.2021.127956
Received 4 October 2021; Received in revised form 16 November 2021; Accepted 28 November 2021
Available online 1 December 2021

decrease in the abundance of white sharks has been observed in other regions, such as the Mediterranean sea (Moro et al., 2020).

White sharks are highly mobile, generalist predators with foraging plasticity encompassing a wide range of prey and habitats (Huveneers et al., 2018). In the north-eastern Pacific (NEP), white sharks perform seasonal migrations from inshore seal colonies to offshore areas where they likely forage on deep mesopelagic prey (Le Croizier et al., 2020a; Jorgensen et al., 2010). In Australian waters, white sharks are divided into two populations, namely the eastern Australasian (EA) and south-western Australasian (SWA) populations (Blower et al., 2012). In the SWA population, although occasional offshore movements were observed, immature and adult sharks mainly occupy coastal waters on the continental shelf where they primarily target locally abundant pinnipeds (Bradford et al., 2020; Bruce et al., 2006; Meyer et al., 2019). Conversely, EA sharks show an ontogenetic (developmental) shift in habitat use, with immature sharks being mainly restricted to coastal waters (Spaet et al., 2020; Bruce et al., 2019) and larger individuals performing wide-spread movements across ocean basins to New Zealand and tropical Pacific islands (Duffy et al., 2012; Bonfil et al., 2010). As the east coast of Australia is devoid of primary seal colonies, coastal fish are the predominant prey for immature EA sharks (Grainger et al., 2020).

Mercury (Hg) is a global pollutant of particular concern to human and wildlife health. Mercury is emitted to the atmosphere from natural and anthropogenic sources and largely deposited to the surface ocean, where a fraction is converted to methylmercury (MeHg) by microorganisms (Driscoll et al., 2013). Methylmercury is characterized by strong neurotoxicity, bioaccumulation in marine biota and unique biomagnification properties in food webs (Kidd et al., 2011). Due to their longevity and high trophic level, white sharks are among the marine species displaying the highest concentrations of Hg, assumed to be predominantly MeHg (Le Croizier et al., 2020a; McKinney et al., 2016). The impact of Hg exposure on shark neurophysiology is still poorly understood (Ehnert-Russo and Gelsleichter, 2020; Rodrigues et al., 2021) and shark species could exhibit metabolic mechanisms allowing them to reduce toxicity, such as in vivo demethylation of MeHg (Le Croizier et al., 2020b). However, the particularly high Hg concentrations found in white sharks likely induce deleterious effects (e.g. damage to the central nervous system, loss of neurons, sensory and motor deficits, oxidative stress) as observed in marine mammals and other shark species (Rodrigues et al., 2021; Krey et al., 2015; López-Berenguer et al., 2020) and represent an additional pressure on this vulnerable species.

In the context of global change, the future trend of Hg concentrations in marine predators remains uncertain. Empirical studies do not reach consensus, as a decrease (Lee et al., 2016; Bank et al., 2021), stability (Médieu et al., 2021; Yurkowski et al., 2020; Renedo et al., 2021) or increase (Drevnick et al., 2015; Dietz et al., 2021; Vo et al., 2011) in predator Hg content has been observed over the past decades, depending on the species and regions considered. Most model projections predict increased Hg levels in meso and top predators under different scenarios of seawater warming and dietary changes due to overfishing of prey stocks (Schartup et al., 2019; Alava et al., 2018; Booth and Zeller, 2005). However, current predictions ignore the foraging plasticity and wide range of ecological traits of apex predators such as white sharks. This could mask the heterogeneity in future contamination patterns within a single species, as individual foraging strategies have been shown to influence Hg exposure and ultimately Hg levels in mesopredators (Peterson et al., 2015). It is therefore essential to characterize and understand intraspecific variability in Hg exposure to better predict the effects of global change on predator contamination and marine ecosystem health.

In recent years, the measurement of the natural abundances of Hg stable isotopes has greatly improved knowledge on the sources of exposure, transfer pathways, and metabolism of Hg in marine consumers (Blum et al., 2013; Renedo et al., 2018; Li et al., 2020). Many abiotic (e.g. photoreduction, volatilization) (Bergquist and Blum, 2007; Zheng et al., 2007) and biotic processes (e.g. methylation, demethylation) (Le Croizier et al., 2020b; Perrot et al., 2016; Janssen et al., 2016) result in mass-dependent isotope fractionation (MDF, reported as δ^{202}Hg), whereas mass-independent fractionation of odd-mass number isotopes (odd-MIF, reported as Δ^{199}Hg or Δ^{201}Hg) has been primarily observed during aquatic photochemical reactions (Bergquist and Blum, 2007). In addition, significant MIF of even-mass number isotopes (even-MIF, reported as Δ^{200}Hg) is thought to occur via Hg photochemistry in the upper atmosphere (Chen et al., 2012). The analysis of Hg isotopes in marine biota therefore provides information about atmospheric Hg deposition pathways to the marine environment (Jiskra et al., 2021), Hg methylation / demethylation processes in the water column and sediments (Tsui et al., 2020), as well as on species biology and ecology, such as Hg metabolism and foraging habitat (Le Croizier et al., 2020a; Le Croizier et al., 2020b). Mercury isotopes have been successfully used to distinguish Hg exposure between sedentary, low trophic level marine fish populations (Cransveld et al., 2017; Pinzone et al., 2021). However, uncertainty remains regarding the possibility of applying this method to assess intraspecific variability in Hg exposure in highly mobile top predators such as white sharks.

To evaluate intraspecific variability in Hg contamination in marine apex predators, we tested the capability of Hg isotopes to identify differences in Hg exposure among three white shark populations (NEP, SWA, and EA) with contrasting ecology and large spatial scales. We discussed the potential links between Hg sources and the known ecological characteristics of these populations. We also sought to describe the dynamics of Hg bioaccumulation within each population. We hypothesized that Hg exposure and levels may vary between populations, making the assessment of Hg fate in marine predators under global change more complex than previously thought.

2. Materials and methods

2.1. Sample collection

2.1.1. North-eastern Pacific population

White sharks (n = 30) were sampled at Guadalupe Island (Mexico) between September and November in 2016, 2017 and 2018 (Fig. 1). Free-swimming white sharks were attracted with bait near the research vessel. Muscle samples were taken using a biopsy probe targeting the tissue directly below the dorsal fin. After collection, samples were immediately transferred to a −20 °C freezer onboard the vessel.

2.1.2. South-western Australasian population

White shark samples (n = 40) were collected from January 2015 to July 2020 at the Neptune Islands Group Marine Park, South Australia (Fig. 1), where free-swimming sharks were targeted opportunistically throughout the year during standard cage-diving operations. Sharks were attracted to the cage-diving vessels using a combination of attractants. Biopsies were taken from diving cages or from the surface using a single 20-mm rubber speargun, with the end of the 1.3 m spear modified into a hollow 1 cm diameter stainless steel biopsy probe (Meyer et al., 2018), targeting the dorsal or upper flank musculature directly below the dorsal fin. Biopsies were immediately frozen (−4 °C) and transported to the laboratory where white muscle tissue was dissected from the sub-dermal tissue and skin.

2.1.3. Eastern Australasian population

White sharks (n = 44) were sampled along the east coast of New South Wales, Australia (within a radius of ~30 km around the town of Ballina, Fig. 1) between 2016 and 2020, using SMART drumlines as part of a bather protection research program (Tate et al., 2021; Tate et al., 2019). After capture, sharks were secured to the side of the vessel and a muscle sample was taken using an 0.8 cm sterile biopsy punch (Kai medical) targeting the tissue directly behind the dorsal fin. Tissue samples were immediately placed into a 5 mL screw cap vial on ice and transferred to a −4 °C freezer.

Individual sharks from all three populations (NEP, SWA, and EA)

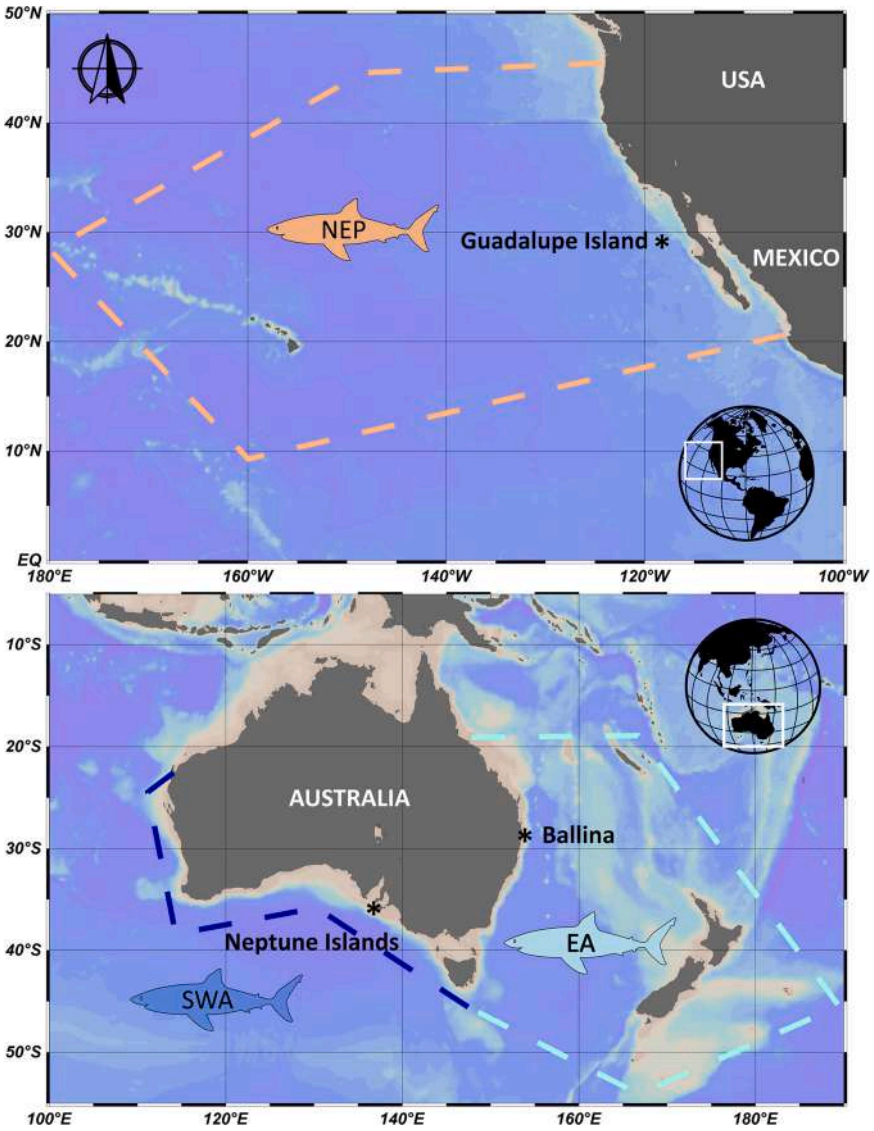

Fig. 1. Map of the spatial distribution of white sharks from the north-eastern Pacific (NEP), eastern Australasian (EA) and south-western Australasian (SWA) populations. Sample collection sites are figured (*).

were sexed (based on clasper presence/absence), and total length was measured to the nearest 10 cm using visual size estimates (NEP and SWA) (May et al., 2019) or to the nearest 1 cm using a certified tape (EA) (Tate et al., 2021; Tate et al., 2019).

2.2. Mercury concentration analysis

Once in the laboratory, muscle samples were lyophilized and homogenized using an electric grinder that was rinsed with alcohol between samples (Fig. S1). Total Hg (THg) concentration was determined on aliquots (around 10 mg) of homogenized samples by combustion, gold trapping and atomic absorption spectrophotometry using a DMA80 analyzer (Milestone, USA). As THg is predominantly in the MeHg form in shark muscle (Le Croizier et al., 2020b; Matulik et al., 2017; Pethybridge et al., 2010a; de Carvalho et al., 2014; Bosch et al., 2016; Nalluri et al., 2014), THg was used as a proxy for MeHg concentration, in accordance with previous studies (Le Croizier et al., 2020a; Besnard et al., 2021). Total Hg concentrations in samples are expressed on a dry weight basis ($\mu g \cdot g^{-1}$ dw). Only one analysis was performed per sample, but the accuracy and reproducibility of the method were established using two freeze-dried certified biological materials: a tuna fish flesh homogenate reference material (IAEA 436, IRMM) and a lobster hepatopancreas reference material (TORT 3, NRCC). The certified values for IAEA 436 (4.19 ± 0.36 $\mu g \cdot g^{-1}$ dw, $n = 10$) were reproduced (measured value: 4.33 ± 0.19 $\mu g \cdot g^{-1}$ dw) within the confidence limits. The certified values for TORT 3 (0.292 ± 0.022 $\mu g \cdot g^{-1}$ dw) were also reproduced (measured value: 0.286 ± 0.024 $\mu g \cdot g^{-1}$ dw, $n = 10$) within the confidence limits. The detection limit was 0.005 $\mu g \cdot g^{-1}$ dw.

2.3. Mercury isotope analysis

Aliquots of approximately 10 mg of dry muscle were left over night (~12 h) at ambient room temperature in 3 mL of concentrated bi-distilled nitric acid (HNO_3). A volume of 1 mL of hydrogen peroxide (H_2O_2) was added, and samples were digested on a hotplate for 6 h at 100 °C. A volume of 100 µL of BrCl was then added to ensure a full conversion of MeHg to inorganic Hg. The digest mixtures were finally diluted in inverse aqua regia (3 HNO_3: 1 HCl, 20 vol% MilliQ water) to reach a nominal Hg concentration of 1 $ng \cdot g^{-1}$. Certified reference materials (ERM-BCR-464) and blanks were prepared in the same way as tissue samples. Mercury isotope composition was measured by multi-collector inductively coupled plasma mass spectrometry (MC−ICP−MS, Thermo Finnigan Neptune Plus) with continuous-flow cold vapor (CV) generation using Sn (II) reduction (CETAC HGX-200).

Mercury isotope ratios are expressed in δ notation and reported in parts per thousand (‰) deviation from the NIST SRM 3133 standard, following sample-standard bracketing according to the following equation: $\delta^{XXX}Hg$ (‰) = [$(^{XXX}Hg/^{198}Hg)_{sample}$ / $(^{XXX}Hg/^{198}Hg)_{NIST\ 3133}$) − 1] X 1000 where xxx represents the mass of each mercury isotope. $\delta^{202}Hg$ represents Hg MDF, and Δ notation is used to express Hg MIF by the following equation:

$$\Delta^{xxx}Hg\ (‰) = \delta^{xxx}Hg - (\delta^{202}Hg \times a)$$

where a = 0.2520, 0.5024 and 0.7520 for isotopes 199, 200 and 201, respectively.

Total Hg in the diluted solutions was quantified by MC-ICP-MS using ^{202}Hg signals: mean recoveries of 98 ± 11% (n = 84) for samples and 96 ± 6 % (n = 12) for certified reference materials were found. Mercury levels in blanks were below the detection limit of 0.005 ng·g^{-1}. Reproducibility of Hg isotope measurements was assessed by analyzing UM-Almadén (n = 24), ETH-Fluka (n = 22) and the biological tissue procedural standard ERM-BCR-464 (n = 12) (Table S1). Measured isotope signatures as well as analytical reproducibility of standards (UM-Almadén, ETH-Fluka and ERM-BCR-464) were found to be in agreement with previously published values (Blum et al., 2013; Masbou et al., 2013; Jiskra et al., 2017) (Table S1). Duplicate analysis was performed on a subset of 15 white shark tissues to assess the analytical uncertainty of $\delta^{202}Hg$ (2 SD = 0.12‰) and $\Delta^{199}Hg$ values (2 SD = 0.10‰) in the samples.

2.4. Data analysis

For comparison of Hg isotope signatures among white shark populations, data were first checked for normality (Shapiro–Wilk tests) and homogeneity of variances (Bartlett tests). One-way analyses of variance (ANOVAs) were applied when these conditions were met, followed by Tukey's HSD tests. In the absence of homoscedasticity, Welch's ANOVAs with Games-Howell post-hoc tests were used. Linear regressions were used to assess relationships between different Hg isotope values, between Hg concentration and shark length, or between Hg isotope values and shark length. Analyses of covariance (ANCOVAs) were used to compare Hg accumulation rates between populations. Generalized linear models (GLMs) were used to evaluate the influence of population, shark length, gender, and Hg isotope values ($\Delta^{200}Hg$, $\Delta^{199}Hg$ and $\delta^{202}Hg$) on Hg levels. Based on the analysis of the residuals, a Gaussian distribution and identity link function were used in the GLMs. The models were built using backward stepwise selection, ranked based on Akaïke's Information Criteria adjusted for small sample sizes (AIC_c) and compared using ΔAIC_c and Akaike weights (w_i). All statistical analyses were performed using the open source software R (4.1.1 version).

3. Results and discussion

3.1. Atmospheric Hg deposition pathways

White shark $\Delta^{200}Hg$ values were close to zero in all three populations (Table 1). The $\Delta^{200}Hg$ signature has previously been used as a conservative tracer of atmospheric Hg deposition pathways (Lepak et al., 2018; Masbou et al., 2018). The deposited Hg subsequently becomes the substrate for MeHg production in marine environments. $\Delta^{200}Hg$ mainly discriminates between dissolution of gaseous Hg(0) (slightly negative $\Delta^{200}Hg$ of −0.05‰) and wet and dry deposition of inorganic Hg(II) through precipitation and dry deposition (positive $\Delta^{200}Hg$ values of 0.14‰) (Enrico et al., 2016). Terrestrial plants and soils have been shown to take up atmospheric Hg(0), and continental runoff by rivers to the oceans thus constitutes an additional Hg source with $\Delta^{200}Hg$ similar to Hg(0) (Obrist et al., 2017). As coastal food webs receive Hg from all three sources, their $\Delta^{200}Hg$ values are generally closer to the Hg(0) than the Hg(II) end-member (Masbou et al., 2018; Meng et al., 2020). Conversely, pelagic ecosystems show equal contributions of Hg(0) and Hg(II) deposition, resulting in $\Delta^{200}Hg$ signatures around 0.05‰ (Lepak et al., 2018; Motta et al., 2019). Here, the mean $\Delta^{200}Hg$ values of 0.06, 0.04, and 0.03‰ for NEP, EA and SWA populations respectively (Table 1) would thus reflect an equivalent contribution of Hg(0) and Hg(II) sources, characteristic of pelagic environments (Jiskra et al., 2021). However, the NEP population displayed a significantly higher $\Delta^{200}Hg$ than the SWA population ($p < 0.05$, Fig. 2A), with EA sharks showing intermediate values. Despite the small magnitude of even-MIF, $\Delta^{200}Hg$ values revealed a greater contribution of Hg(II) inputs in the NEP population compared to SWA sharks. This hypothesis agrees with a previous study showing that NEP white sharks were dietary exposed to mesopelagic MeHg (Le Croizier et al., 2020a), which is mainly produced from Hg(II) supplied by precipitation and dry deposition in the subtropical Pacific (Motta et al., 2019). Although Hg isotope signatures of prey have not yet been characterized for Australasian sharks, movement data showed that SWA sharks primarily occupy coastal waters (Bradford et al., 2020; Bruce et al., 2006) (Table 1), which are believed to receive more Hg(0) inputs via continental runoff. The coastal affinity of SWA sharks, opposed to the pelagic foraging behavior of NEP sharks, could thus explain the variations in $\Delta^{200}Hg$ observed between these populations (i.e. higher $\Delta^{200}Hg$ in NEP sharks, Fig. 2A).

A recent global analysis of marine $\Delta^{200}Hg$ (including particulate Hg, sediments, and biota) showed the occurrence of a latitudinal isotopic gradient, with lower $\Delta^{200}Hg$ values at high latitudes, indicating larger ocean Hg(0) uptake compared to intermediate and tropical areas (Jiskra et al., 2021). However, this study reported similar $\Delta^{200}Hg$ values at the latitudes corresponding to our sampling sites, i.e., around 30°N and 30°S (Fig. 1). The variability in $\Delta^{200}Hg$ observed in our study seems to be governed by differences in atmospheric Hg sources between coastal and offshore shark habitats, rather than by a latitudinal gradient in $\Delta^{200}Hg$ at the global scale.

4. Marine MeHg sources

Mercury odd-MIF signatures in marine biota are not affected by trophic transfers or metabolic processes (Perrot et al., 2016; Kwon et al., 2012) and are specifically derived from the photodegradation of MeHg in seawater prior to food web biomagnification (Blum et al., 2013). Although similar $\Delta^{201}Hg/\Delta^{199}Hg$ ratios across regions suggest a common mechanism for MeHg photodegradation (Fig. S2 and additional

Table 1
Summary of Hg analyses (mean ± standard deviation) carried out in white shark muscle. Shark length is indicated as mean (range). Habitat characteristics are reported according to previous studies (Jorgensen et al., 2010; He et al., 2017; Bradford et al., 2020; Spaet et al., 2020).

Population	n	Total length (m)	Maturity stage	THg (μg·g^{-1})	$\delta^{202}Hg$ (‰)	$\Delta^{199}Hg$ (‰)	$\Delta^{200}Hg$ (‰)	Vertical habitat	Horizontal habitat	Secchi depth
North-eastern Pacific (NEP)	30	3.1 (2.0–5.0)	Juvenile to adult	10.58 ± 2.64	0.88 ± 0.25	1.54 ± 0.18	0.06 ± 0.03	Epi to mesopelagic	In to offshore	50
Eastern Australasian (EA)	44	2.4 (1.6–3.5)	Juvenile to subadult	10.50 ± 5.51	0.92 ± 0.25	1.25 ± 0.19	0.04 ± 0.05	Epipelagic	Continental shelf	30
South-western Australasian (SWA)	40	3.2 (1.8–4.7)	Juvenile to adult	18.31 ± 8.08	1.43 ± 0.40	1.69 ± 0.19	0.03 ± 0.05	Epipelagic	Continental shelf	30

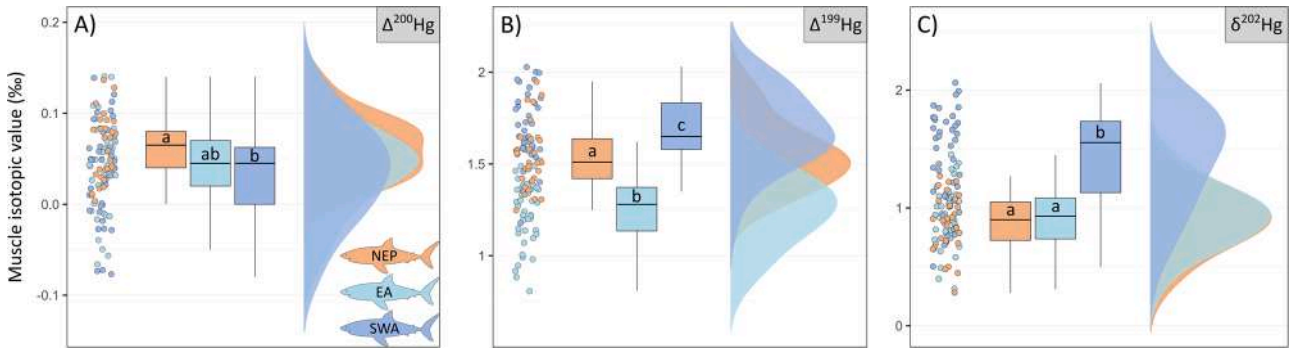

Fig. 2. Raw data points, boxplots and data distribution of A) Δ^{200}Hg, B) Δ^{199}Hg and C) δ^{202}Hg values in the muscle of different white shark populations: the north-eastern Pacific (NEP), eastern Australasian (EA) and south-western Australasian (SWA) populations. Different letters indicate significant differences between populations (ANOVAs; $p < 0.05$).

discussion), we found significant variations in Δ^{199}Hg values between populations ($p < 0.01$, Fig. 2B), indicating exposure to distinct MeHg pools that experienced different intensities of photodegradation. In the open ocean or near offshore islands, where marine organisms are mainly exposed to pelagic MeHg, fish species are characterized by Δ^{199}Hg values generally higher than 1‰ (Le Croizier et al., 2020b; Blum et al., 2013; Sackett et al., 2017). Conversely, marine fishes exposed to MeHg produced in coastal sediments or turbid waters, where light penetration is limited, display significantly lower Δ^{199}Hg values (typically lying between 0‰ and 1‰) (Meng et al., 2020; Senn et al., 2010; Perrot et al., 2019). In addition, as Hg photodegradation decreases with light attenuation in the water column, Δ^{199}Hg values generally decrease with increasing foraging depth in marine fishes (Blum et al., 2013; Le Croizier et al., 2020b; Sackett et al., 2017). Δ^{199}Hg values in a marine predator may thus reflect vertical or horizontal habitat use, or a combination of both, depending on the environment considered (Sun et al., 2021). As it was previously shown that NEP sharks are primarily exposed to deep and offshore MeHg (Le Croizier et al., 2020a), and SWA and EA sharks occupy mainly coastal and shallow habitats (Bradford et al., 2020; Bruce et al., 2006; Spaet et al., 2020; Bruce et al., 2019), Δ^{199}Hg signatures were expected to differ between NEP and Australasian populations, as observed in our dataset (Fig. 2B). Surprisingly, the NEP population showed a Δ^{199}Hg of 1.54‰, which fell between the Δ^{199}Hg of SWA and EA populations (1.69 and 1.25‰, respectively) (Table 1). Photochemical degradation of MeHg in epipelagic layers is known to vary globally, primarily related to water clarity and UV penetration depth (Motta et al., 2020). Differences in habitat characteristics and water clarity (based on Secchi depth; Table 1) therefore suggest variations in Δ^{199}Hg baselines across distant regions, complicating direct comparison of NEP and Australasian populations. By focusing on spatially close populations, a gap in Δ^{199}Hg values was also observed between SWA and EA sharks, despite an apparent similarity in vertical and horizontal habitat use for the size classes considered (Bradford et al., 2020; Bruce et al., 2006; Spaet et al., 2020; Bruce et al., 2019), and in average water clarity in both regions (He et al., 2017) (Table 1). However, when closely examining the fine-scale distribution in the water column, SWA sharks were observed to primarily occupy the upper 50 m (Bradford et al., 2020), while EA sharks were most abundant between 50 and 130 m depth (Lee et al., 2021). As the MeHg photodegradation gradient is steep in shallow depths (Blum et al., 2013; Le Croizier et al., 2020a), this inconspicuous but significant difference in vertical habitat is consistent with the Δ^{199}Hg variation observed between Australasian (SWA and EA) populations. This exemplifies the ability and sensitivity of the Δ^{199}Hg tracer to capture slight variations in vertical habitat used by nearby predator populations.

Although many biotic and abiotic processes affect Hg MDF, hepatic MeHg demethylation has been identified as one of the major mechanisms leading to increased δ^{202}Hg values in the muscle tissue of predators such as marine mammals (Li et al., 2020; Perrot et al., 2016), seabirds (Poulin et al., 2021; Renedo et al., 2021), and sharks (Le Croizier et al., 2020b; Besnard et al., 2021). The preferential demethylation of light Hg isotopes in the liver increases δ^{202}Hg in the remaining MeHg pool, a fraction of which is ultimately stored in muscle (Perrot et al., 2016; Poulin et al., 2021). Here, we found high δ^{202}Hg values (up to 1.43‰ in the SWA population; Table 1) and near zero Δ^{199}Hg/δ^{202}Hg slopes (Fig. S3 and additional discussion) which may suggest substantial MeHg demethylation in white sharks, as previously established for other large species such as bull and tiger sharks (Le Croizier et al., 2020b). Alternatively, it may result from the consumption of marine mammals, which can represent an important part of the white shark diet (Grainger et al., 2020; Hussey et al., 2012) and which also display elevated δ^{202}Hg values due to MeHg demethylation (Perrot et al., 2016; Bolea-Fernández et al., 2019). The higher δ^{202}Hg found in SWA sharks compared to the NEP and EA populations (Fig. 2) could thus be the result of either higher demethylation or more frequent consumption of marine mammals. In our study, SWA sharks had much higher Hg concentrations than NEP sharks (Table 1), which does not support the hypothesis of higher demethylation. However, the second hypothesis is supported by the modest contribution of mammals to Hg exposure of NEP sharks (Le Croizier et al., 2020a) and dietary intake of immature EA sharks (Grainger et al., 2020), while the SWA shark samples were collected near a large colony of pinnipeds (Neptune Islands Group Marine Park; Fig. 1).

5. Individual variability in Hg exposure

No variation in Hg isotope signatures related to gender or body length has been previously found in NEP sharks, suggesting a common Hg exposure at the population scale (Le Croizier et al., 2020a). Conversely, ontogenetic variability was observed here within the two Australasian populations. In the EA population, Δ^{199}Hg was positively correlated with shark total length (Fig. 3A). Previous studies of the EA white shark population have shown an ontogenetic increase in travelling behavior (Lee et al., 2021), with coastal areas dominated by small immature individuals (Spaet et al., 2020; Bruce et al., 2019; Grainger et al., 2020; Spaet et al., 2020) and large sharks more likely to undertake large-scale offshore migrations (Duffy et al., 2012; Bonfil et al., 2010; Francis et al., 2015). Such an increase in offshore dispersal would result in greater exposure to pelagic MeHg sources, typically characterized by higher Δ^{199}Hg values (Le Croizier et al., 2020b; Blum et al., 2013; Sackett et al., 2017) than MeHg produced in coastal habitats (Meng et al., 2020; Senn et al., 2010; Perrot et al., 2019), and would explain the ontogenetic variation in Δ^{199}Hg found in EA sharks.

In SWA sharks, both δ^{202}Hg and Δ^{200}Hg were found to increase with size (Figs. 3B, 3C). Mercury metabolism in sharks is supposed to increase δ^{202}Hg values over time, through enhanced MeHg demethylation in

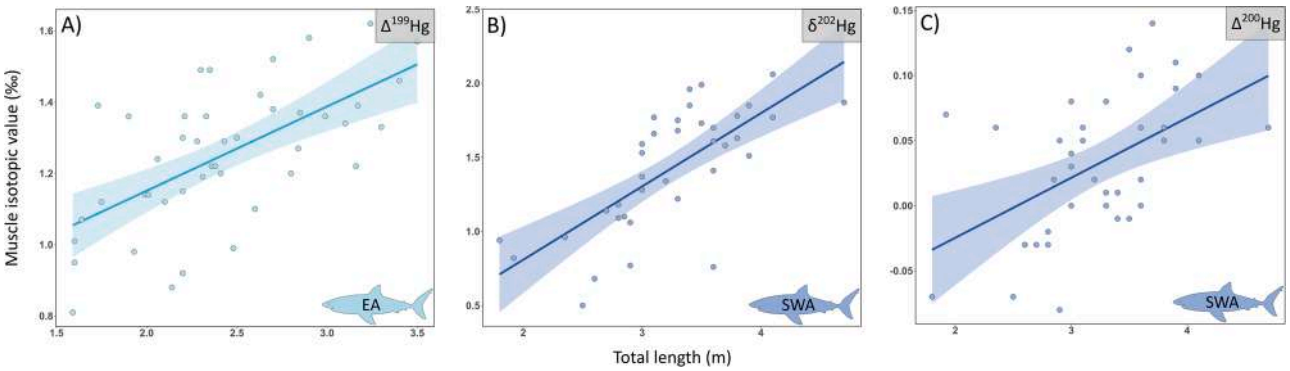

Fig. 3. Relationships between A) Δ^{199}Hg, B) δ^{202}Hg and C) Δ^{200}Hg values and body length in the eastern Australasian (EA) and south-western Australasian (SWA) populations. Data fits a linear regression in A) $R^2 = 0.40$, $p < 0.001$; B) $R^2 = 0.49$, $p < 0.001$ and C) $R^2 = 0.26$, $p < 0.01$.

older individuals (Le Croizier et al., 2020b). In addition, white sharks are known to increase their consumption of marine mammals as they grow larger (Hussey et al., 2012), which may increase the uptake of MeHg with δ^{202}Hg higher values (Le Croizier et al., 2020a). It is therefore difficult to deconvolute the different mechanisms (Hg metabolism, change in prey) responsible for ontogenetic variations in the δ^{202}Hg signature. However, as δ^{202}Hg values did not increased with size in NEP and EA populations, changes in δ^{202}Hg are unlikely to be caused by metabolism alone. Considering that oceanic Δ^{200}Hg baselines are generally slightly higher than coastal baselines (Lepak et al., 2018; Meng et al., 2020; Motta et al., 2019), the higher Δ^{200}Hg observed in large SWA sharks suggests an ontogenetic increase in offshore movements in this population. This is consistent with a recent tracking study documenting movements of large SWA sharks (> 4.5 m) off the continental shelf and suggesting that females may disperse further offshore than males (Bradford et al., 2020). While we did not observe differences in Hg exposure between sexes, Δ^{200}Hg values provide evidence for an ontogenetic change in foraging habitat in the SWA population.

6. Mercury bioaccumulation

Log-transformed THg concentrations were positively correlated with shark length (a proxy for age) in Australasian sharks (Fig. 4) and the log (THg)/length slopes were similar in SWA and EA populations (ANCOVA, $p > 0.05$). These results indicate a comparable rate of Hg bioaccumulation in the two Australasian populations. Methylmercury bioaccumulation in fish muscle results from a high MeHg assimilation efficiency, strong binding to cysteine residues of proteins and low excretion rate (Wang and Wong, 2003; Manceau et al., 2021). Moreover, MeHg stored in muscle comes from the residual blood MeHg exiting from the liver after in vivo demethylation. As MeHg is the dominant form of Hg in shark muscle (Le Croizier et al., 2020b; Matulik et al., 2017; de Carvalho et al., 2014), increased Hg concentration in the muscle of Australasian sharks may imply that trophic exposure to MeHg exceeds demethylation capacity. Our findings are consistent with a previous study which observed an increase in Hg concentration with size in juvenile EA individuals (Gilbert et al., 2015). In contrast, no increase in Hg concentration with age was observed in NEP sharks (Fig. 4), suggesting a balance between MeHg exposure and demethylation/excretion. Consequently, while Hg concentrations were similar in all three populations for smaller sharks (i.e., 11 and 12 $\mu g \cdot g^{-1}$ dw at 2.5 m total length for Australasian and NEP sharks, respectively), Australasian populations were three times more contaminated than the NEP population for larger sharks (e.g., 30 versus 10 $\mu g \cdot g^{-1}$ dw at 4.5 m total length for SWA and NEP sharks, respectively; Fig. S4).

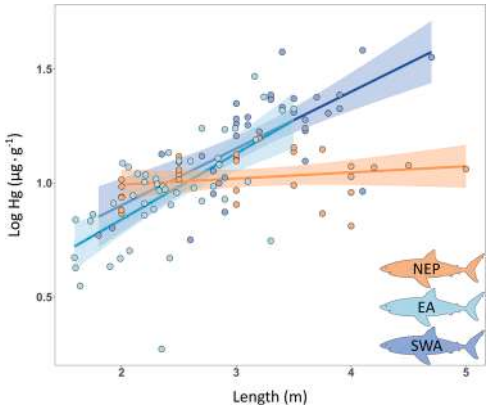

Fig. 4. Relationships between log-transformed Hg concentration and total length (m) in the muscle of different white shark populations: the north-eastern Pacific (NEP), eastern Australasian (EA) and south-western Australasian (SWA) populations. Data fits a linear regression in the EA (R^2 =0.41, $p < 0.001$) and SWA (R^2 =0.50, $p < 0.001$) populations, but not in the NEP population ($p > 0.05$).

Similar muscle Hg concentrations observed in young white sharks do not argue for variations in marine MeHg baselines across regions. However, the difference in Hg accumulation kinetics found between Australasian and NEP populations (Fig. 4) could be related to different trophic strategies adopted by adult sharks. While δ^{202}Hg values suggest a size-based increase in MeHg uptake from marine mammals consumption in SWA sharks (Fig. 3B), the NEP population is thought to be primarily exposed to MeHg from mesopelagic prey with limited contribution from pinnipeds, regardless of size (Le Croizier et al., 2020a). As predators, marine mammals generally display higher Hg content than mid-trophic mesopelagic species (Kemper et al., 1994; Pethybridge et al., 2010b). A greater proportion of mammals in the diet of adult SWA sharks could thus partly explain their higher δ^{202}Hg values and Hg concentrations compared to the NEP population. This assumption is consistent with the outputs of generalized linear models used to predict Hg levels in white shark muscle. The top-ranked model ($w_i = 0.60$) included δ^{202}Hg, length and population, and δ^{202}Hg was the best stand-alone predictor of Hg concentration, explaining 36% of Hg variation in shark muscle (Table S2). This result revealed that consumption of marine mammals (exhibiting high δ^{202}Hg values (Le Croizier et al., 2020a) could be a major driver of Hg levels in white sharks. In the future, this hypothesis can be verified by comparing the trophic level of adult sharks from the NEP and Australasian populations, but may require the use of amino acid nitrogen isotopic analysis to overcome spatial variations in isotopic baselines (Ohkouchi et al., 2017).

7. Conclusion

Global change is expected to influence Hg contamination in marine biota, yet intra-species differences in Hg exposure are rarely considered. Here, we applied for the first time the recent technique of Hg isotope

analysis to characterize dietary Hg exposure across different populations of white sharks, the world's largest predatory fish. Our results revealed that the broad ecological spectrum of white sharks implies exposure to different sources of Hg among individuals, likely leading to the marked differences in Hg bioaccumulation patterns observed between populations. Given this large intraspecific variability, predicting Hg levels in marine predators under global change could be more complex than previously thought. Future modelling research should therefore focus on a widely distributed top predator model species and account for population variations in Hg exposure and concentration to improve projections of predator Hg levels at the global scale.

CRediT authorship contribution statement

Gaël Le Croizier: Conceptualization, Methodology, Formal analysis, Writing – original draft, Writing – review & editing. **Jeroen Sonke**: Formal analysis, Resources, Writing – review & editing, Supervision, Funding acquisition. **Anne Lorrain** Resources, Writing – review & editing, Supervision, Funding acquisition. **Marina Renedo**: Formal analysis, Writing – review & editing. **Mauricio Hoyos-Padilla**: Investigation, Resources, Writing – review & editing, Funding acquisition. **Omar Santana-Morales**: Investigation, Resources, Writing – review & editing, Funding acquisition. **Lauren Meyer**: Investigation, Resources, Writing – review & editing, Funding acquisition. **Charlie Huveneers**: Investigation, Resources, Writing – review & editing, Funding acquisition. **Paul Butcher**: Investigation, Resources, Writing – review & editing, Funding acquisition. **Felipe Amezcua-Martinez**: Writing – review & editing. **David Point**: Resources, Writing – review & editing, Supervision, Funding acquisition.

Declaration of Competing Interest

The authors declare that they have no known competing financial interests or personal relationships that could have appeared to influence the work reported in this paper.

Acknowledgments

Gaël Le Croizier was supported by a postdoctoral grant from the French National Research Institute for Sustainable Development (IRD) and the ISblue "Interdisciplinary graduate School for the blue planet" project (ANR-17-EURE-0015). We thank the French National Research Agency ANR-17-CE34-0010 project 'Unraveling the origin of methylMERcury TOXin in marine ecosystems' (MERTOX, PI DP) for providing financial support for Hg isotope analysis. The project was funded in Mexico by Alianza WWF-TELCEL, The Annemberg Foundation, International Community Foundation, Fins Attached Marine Research and Conservation and Pfleger Institute of Environmental Research. Field work in Mexico was greatly facilitated through courtesies extended to us by personnel of the University of California, Davis, Centro Interdisciplinario de Ciencias Marinas (CICIMAR), Secretaría de Marina, Comisión de Areas naturals Protegidas (CONANP), Island Conservation (GECI), Horizon Charters, Islander Charters, Solmar V, Club Cantamar and local fishermen from Guadalupe Island. In Mexico, white shark samples were collected under permits from the Secretaría del Medio Ambiente y Recursos Naturales (SEMARNAT): OFICIO NUM.SGPA/DGVS/07052/16 in 2016, OFICIO NUM.SGPA/DGVS/06673/17 in 2017 and OFICIO NUM.SGPA/DGVS/004284/18 in 2018. Fieldwork in South Australia was possible thanks to the logistic support of the white shark cage-diving industry. We also thank the Save Our Seas Foundation, Holsworth Wildlife Research Endowment (HWRE2016R2098), Oceania Chondrichthyan Society and Passions of Paradise for providing funding to support sample collection. In South Australia, samples were collected in accordance with DEWNR permit #Q26292 and Flinders University Animal Ethics Committee approval #398 for South Australian samples. In New South Wales (NSW), samples were collected by the NSW DPI shark research team and SMART drumline contractors. NSW samples were collected under NSW DPI 'scientific' (Ref. P01/0059(A)), 'Marine Parks' (Ref. P16/0145-1.1) and 'Animal Care and Ethics' (ACEC Ref. 07/08) permits as part of the Shark Management Strategy. We also thank Jonathan Werry for his contribution to shark sampling in Eastern Australia. White shark samples were exported from Mexico under the CITES permit (number MX007) of the Universidad Nacional Autónoma de México and from Australia under the CITES permit (number AU089) of Flinders University. Samples were imported in France under the CITES permit (number FR75A) of the Muséum National d'Histoire Naturelle. We thank Laure Laffont and Jérôme Chmeleff for expert management of the OMP mercury and mass spectrometry facilities.

Appendix A. Supporting information

Supplementary data associated with this article can be found in the online version at doi:10.1016/j.jhazmat.2021.127956.

References

Alava, J.J., Cisneros-Montemayor, A.M., Sumaila, U.R., Cheung, W.W.L., 2018. Projected amplification of food web bioaccumulation of MeHg and PCBs under climate change in the Northeastern Pacific. Sci. Rep. 8 (1), 13460. https://doi.org/10.1038/s41598-018-31824-5.

Bank, M.S.;, Frantzen, S.;, Duinker, A.;, Amouroux, D.;, Tessier, E.;, Nedreaas, K.;, Maage, A.;, Nilsen, B.M., 2021. Rapid temporal decline of mercury in Greenland Halibut (Reinhardtius hippoglossoides). Environ. Pollut. 289, 117843 https://doi.org/10.1016/j.envpol.2021.117843.

Baum, J.K., Myers, R.A., Kehler, D.G., Worm, B., Harley, S.J., Doherty, P.A., 2003. Collapse and conservation of shark populations in the Northwest Atlantic. Science 299 (5605), 389–392. https://doi.org/10.1126/science.1079777.

Bergquist, B.A., Blum, J.D., 2007. Mass-dependent and -independent fractionation of Hg isotopes by photoreduction in aquatic systems. Science 318 (5849), 417–420. https://doi.org/10.1126/science.1148050.

Besnard, L., Le Croizier, G., Galván-Magaña, F., Point, D., Kraffe, E., Ketchum, J., Martinez Rincon, R.O., Schaal, G., 2021. Foraging depth depicts resource partitioning and contamination level in a Pelagic Shark assemblage: insights from mercury stable isotopes. Environ. Pollut., 117066 https://doi.org/10.1016/j.envpol.2021.117066.

Blower, D.C., Pandolfi, J.M., Bruce, B.D., Gomez-Cabrera, M., del, C., Ovenden, J.R., 2012. Population genetics of Australian White Sharks reveals fine-scale spatial structure, transoceanic dispersal events and low effective population sizes. Mar. Ecol. Prog. Ser. 455, 229–244. https://doi.org/10.3354/meps09659.

Blum, J.D., Popp, B.N., Drazen, J.C., Anela Choy, C., Johnson, M.W., 2013. Methylmercury production below the mixed layer in the North Pacific Ocean. Nat. Geosci. 6 (10), 879–884. https://doi.org/10.1038/ngeo1918.

Bolea-Fernández, E.;, Rua-Ibarz, A.;, Krupp, E.;, Feldmann, J.;, Vanhaecke, F., 2019. High-precision isotopic analysis sheds new light on mercury metabolism in long-finned pilot whales (Globicephala melas). Sci. Rep. 9 https://doi.org/10.1038/s41598-019-43825-z.

Bonfil, R., Francis, M.P., Duffy, C., Manning, M.J., O'Brien, S., 2010. Large-scale tropical movements and diving behavior of white sharks Carcharodon carcharias tagged off New Zealand. Aquat. Biol. 8 (2), 115–123. https://doi.org/10.3354/ab00217.

Booth, S., Zeller, D., 2005. Mercury, food webs, and marine mammals: implications of diet and climate change for human health. Environ. Health Perspect. 113 (5), 521–526. https://doi.org/10.1289/ehp.7603.

Bosch, A.C., O'Neill, B., Sigge, G.O., Kerwath, S.E., Hoffman, L.C., 2016. Heavy metal accumulation and toxicity in smoothhound (Mustelus mustelus) shark from Langebaan Lagoon, South Africa. Food Chem. 190, 871–878. https://doi.org/10.1016/j.foodchem.2015.06.034.

Bradford, R., Patterson, T.A., Rogers, P.J., McAuley, R., Mountford, S., Huveneers, C., Robbins, R., Fox, A., Bruce, B.D., 2020. Evidence of diverse movement strategies and habitat use by white sharks, Carcharodon carcharias, off Southern Australia. Mar. Biol. 167 (7), 96. https://doi.org/10.1007/s00227-020-03712-y.

Bruce, B.D.; Stevens, J.D.; Malcolm, H. Movements and Swimming Behaviour of White Sharks (Carcharodon carcharias) in Australian Waters | Bycatch Management Information System (BMIS). http://link.springer.com/article/10.1007/s00227–006-0325–1 2006. https://doi.org/10.1007/s00227–006-0325–1.

Bruce, B.D., Harasti, D., Lee, K., Gallen, C., Bradford, R., 2019. Broad-Scale Movements of Juvenile White Sharks Carcharodon carcharias in Eastern Australia from Acoustic and Satellite Telemetry. Mar. Ecol. Prog. Ser. 619, 1–15. https://doi.org/10.3354/meps12969.

de Carvalho, G.G.A., Degaspari, I.A.M., Branco, V., Canário, J., de Amorim, A.F., Kennedy, V.H., Ferreira, J.R., 2014. Assessment of Total and Organic Mercury Levels in Blue Sharks (Prionace glauca) from the South and Southeastern Brazilian Coast. Biol. Trace Elem. Res 159 (1), 128–134. https://doi.org/10.1007/s12011-014-9995-6.

Chen, J., Hintelmann, H., Feng, X., Dimock, B., 2012. Unusual Fractionation of Both Odd and Even Mercury Isotopes in Precipitation from Peterborough, ON, Canada.

Geochim. Et. Cosmochim. Acta 90, 33–46. https://doi.org/10.1016/j.gca.2012.05.005.
Cransveld, A., Amouroux, D., Tessier, E., Koutrakis, E., Ozturk, A.A., Bettoso, N., Mieiro, C.L., Bérail, S., Barre, J.P.G., Sturaro, N., Schnitzler, J., Das, K., 2017. Mercury Stable Isotopes Discriminate Different Populations of European Seabass and Trace Potential Hg Sources around Europe. Environ. Sci. Technol. 51 (21), 12219–12228. https://doi.org/10.1021/acs.est.7b01307.
Davenport, D., Butcher, P., Andreotti, S., Matthee, C., Jones, A., Ovenden, J., 2021. Effective Number of White Shark (Carcharodon carcharias, Linnaeus) Breeders Is Stable over Four Successive Years in the Population Adjacent to Eastern Australia and New Zealand. Ecol. Evol. 11 (1), 186–198. https://doi.org/10.1002/ece3.7007.
Dietz, R., Desforges, J.-P., Rigét, F.F., Aubail, A., Garde, E., Ambus, P., Drimmie, R., Heide-Jørgensen, M.P., Sonne, C., 2021. Analysis of narwhal tusks reveals lifelong feeding ecology and mercury exposure. Curr. Biol. https://doi.org/10.1016/j.cub.2021.02.018.
Drevnick, P.E., Lamborg, C.H., Horgan, M.J., 2015. Increase in Mercury in Pacific Yellowfin Tuna. Environ. Toxicol. Chem. 34 (4), 931–934. https://doi.org/10.1002/etc.2883.
Driscoll, C.T., Mason, R.P., Chan, H.M., Jacob, D.J., Pirrone, N., 2013. Mercury as a Global Pollutant: Sources, Pathways, and Effects. Environ. Sci. Technol. 47 (10), 4967–4983. https://doi.org/10.1021/es305071v.
Duffy, C.A., Francis, M.P., Manning, M.J., Bonfil, R., 2012. Regional Population Connectivity, Oceanic Habitat, and Return Migration Revealed by Satellite Tagging of White Sharks, Carcharodon carcharias, at New Zealand Aggregation Sites. Glob. Perspect. Biol. life Hist. White shark 301–318.
Dulvy, N.K., Pacoureau, N., Rigby, C.L., Pollom, R.A., Jabado, R.W., Ebert, D.A., Finucci, B., Pollock, C.M., Cheok, J., Derrick, D.H., Herman, K.B., Sherman, C.S., VanderWright, W.J., Lawson, J.M., Walls, R.H.L., Carlson, J.K., Charvet, P., Bineesh, K.K., Fernando, D., Ralph, G.M., Matsushiba, J.H., Hilton-Taylor, C., Fordham, S.V., Simpfendorfer, C.A., 2021. Overfishing Drives over One-Third of All Sharks and Rays toward a Global Extinction Crisis. Curr. Biol. https://doi.org/10.1016/j.cub.2021.08.062.
Ehnert-Russo, S.L.;, Gelsleichter, J., 2020. Mercury Accumulation and Effects in the Brain of the Atlantic Sharpnose Shark (Rhizoprionodon terraenovae). Arch. Environ. Contam. Toxicol. 78 (2), 267–283. https://doi.org/10.1007/s00244-019-00691-0.
Enrico, M., Roux, G.L., Marusczak, N., Heimbürger, L.-E., Claustres, A., Fu, X., Sun, R., Sonke, J.E., 2016. Atmospheric Mercury Transfer to Peat Bogs Dominated by Gaseous Elemental Mercury Dry Deposition. Environ. Sci. Technol. 50 (5), 2405–2412. https://doi.org/10.1021/acs.est.5b06058.
Ferretti, F., Worm, B., Britten, G.L., Heithaus, M.R., Lotze, H.K., 2010. Patterns and Ecosystem Consequences of Shark Declines in the Ocean. Ecol. Lett. 13 (8), 1055–1071. https://doi.org/10.1111/j.1461-0248.2010.01489.x.
Ferretti, F., Curnick, D., Liu, K., Romanov, E.V., Block, B.A., 2018. Shark Baselines and the Conservation Role of Remote Coral Reef Ecosystems. Sci. Adv. 4 (3), eaaq0333. https://doi.org/10.1126/sciadv.aaq0333.
Francis, M.P., Duffy, C., Lyon, W., Francis, M.P., Duffy, C., Lyon, W., 2015. Spatial and Temporal Habitat Use by White Sharks (Carcharodon carcharias) at an Aggregation Site in Southern New Zealand. Mar. Freshw. Res. 66 (10), 900–918. https://doi.org/10.1071/MF14186.
Gilbert, J.M., Reichelt-Brushett, A.J., Butcher, P.A., McGrath, S.P., Peddemors, V.M., Bowling, A.C., Christidis, L., 2015. Metal and Metalloid Concentrations in the Tissues of Dusky Carcharhinus obscurus, Sandbar C. Plumbeus and White Carcharodon carcharias Sharks from South-Eastern Australian Waters, and the Implications for Human Consumption. Mar. Pollut. Bull. 92 (1), 186–194. https://doi.org/10.1016/j.marpolbul.2014.12.037.
Grainger, R.;, Peddemors, V.M.;, Raubenheimer, D.;, Machovsky-Capuska, G.E., 2020. Diet Composition and Nutritional Niche Breadth Variability in Juvenile White Sharks (Carcharodon carcharias). Front. Mar. Sci. 7 https://doi.org/10.3389/fmars.2020.00422.
He, X., Pan, D., Bai, Y., Wang, T., Chen, C.-T.A., Zhu, Q., Hao, Z., Gong, F., 2017. Recent Changes of Global Ocean Transparency Observed by SeaWiFS. Cont. Shelf Res. 143, 159–166. https://doi.org/10.1016/j.csr.2016.09.011.
Heithaus, M.R., Frid, A., Wirsing, A.J., Worm, B., 2008. Predicting Ecological Consequences of Marine Top Predator Declines. Trends Ecol. Evol. 23 (4), 202–210. https://doi.org/10.1016/j.tree.2008.01.003.
Hussey, N.E., McCann, H.M., Cliff, G., Dudley, S.F., Wintner, S.P., Fisk, A.T., 2012. Size-Based Analysis of Diet and Trophic Position of the White Shark (Carcharodon carcharias) in South African Waters. In: Domeier, M.L. (Ed.), *Global Perspectives on the Biology and Life History of the* White Shark', pp. 27–49.
Huveneers, C., Apps, K., Becerril-García, E.E., Bruce, B., Butcher, P.A., Carlisle, A.B., Chapple, T.K., Christiansen, H.M., Cliff, G., Curtis, T.H., Daly-Engel, T.S., Dewar, H., Dicken, M.L., Domeier, M.L., Duffy, C.A.J., Ford, R., Francis, M.P., French, G.C.A., Galván-Magaña, F., García-Rodríguez, E., Gennari, E., Graham, B., Hayden, B., Hoyos-Padilla, E.M., Hussey, N.E., Jewell, O.J.D., Jorgensen, S.J., Kock, A.A., Lowe, C.G., Lyons, K., Meyer, L., Oelofse, G., Oñate-González, E.C., Oosthuizen, H., O'Sullivan, J.B., Ramm, K., Skomal, G., Sloan, S., Smale, M.J., Sosa-Nishizaki, O., Sperone, E., Tamburin, E., Towner, A.V., Wcisel, M.A., Weng, K.C., Werry, J.M., 2018. Future Research Directions on the "Elusive" White Shark. Front. Mar. Sci. 5 https://doi.org/10.3389/fmars.2018.00455.
Janssen, S.E., Schaefer, J.K., Barkay, T., Reinfelder, J.R., 2016. Fractionation of Mercury Stable Isotopes during Microbial Methylmercury Production by Iron- and Sulfate-Reducing Bacteria. Environ. Sci. Technol. 50 (15), 8077–8083. https://doi.org/10.1021/acs.est.6b00854.
Jiskra, M., Heimbürger-Boavida, L.-E., Desgranges, M.-M., Petrova, M.V., Dufour, A., Ferreira-Araujo, B., Masbou, J., Chmeleff, J., Thyssen, M., Point, D., Sonke, J.E., 2021. Mercury Stable Isotopes Constrain Atmospheric Sources to the Ocean. Nature 597 (7878), 678–682. https://doi.org/10.1038/s41586-021-03859-8.
Jiskra, M.; G., Wiederhold, J.;, Skyllberg, U.;, Kronberg, R.-M.;, Kretzschmar, R., 2017. Source Tracing of Natural Organic Matter Bound Mercury in Boreal Forest Runoff with Mercury Stable Isotopes. Environ. Sci.: Process. Impacts 19 (10), 1235–1248. https://doi.org/10.1039/C7EM00245A.
Jorgensen, S.J., Reeb, C.A., Chapple, T.K., Anderson, S., Perle, C., Van Sommeran, S.R., Fritz-Cope, C., Brown, A.C., Klimley, A.P., Block, B.A., 2010. Philopatry and Migration of Pacific White Sharks. Proc. R. Soc. B: Biol. Sci. 277 (1682), 679–688. https://doi.org/10.1098/rspb.2009.1155.
Kemper, C., Gibbs, P., Obendorf, D., Marvanek, S., Lenghaus, C., 1994. A Review of Heavy Metal and Organochlorine Levels in Marine Mammals in Australia. Sci. Total Environ. 154 (2), 129–139. https://doi.org/10.1016/0048-9697(94)90083-3.
Kidd, K., Clayden, M., Jardine, T., 2011. Bioaccumulation and Biomagnification of Mercury through Food Webs. In *Environmental Chemistry and Toxicology of Mercury*; John Wiley & Sons. Ltd 453–499. https://doi.org/10.1002/9781118146644.ch14.
Krey, A., Ostertag, S.K., Chan, H.M., 2015. Assessment of Neurotoxic Effects of Mercury in Beluga Whales (Delphinapterus leucas), Ringed Seals (Pusa hispida), and Polar Bears (Ursus maritimus) from the Canadian Arctic. Sci. Total Environ. 509–510, 237–247. https://doi.org/10.1016/j.scitotenv.2014.05.134.
Kwon, S.Y., Blum, J.D., Carvan, M.J., Basu, N., Head, J.A., Madenjian, C.P., David, S.R., 2012. Absence of Fractionation of Mercury Isotopes during Trophic Transfer of Methylmercury to Freshwater Fish in Captivity. Environ. Sci. Technol. 46 (14), 7527–7534. https://doi.org/10.1021/es300794q.
Le Croizier, G., Lorrain, A., Sonke, J.E., Hoyos-Padilla, M., Galván-Magaña, F., Santana-Morales, O., Aquino-Baleyto, M., Becerril-García, E., Muntaner López, G., Block, B., Carlisle, A., Jorgensen, S., Besnard, L., Jung, A., Schaal, G., Point, D., 2020a. The Twilight Zone as a Major Foraging Habitat and Mercury Source for the Great White Shark. Environ. Sci. Technol. https://doi.org/10.1021/acs.est.0c05621.
Le Croizier, G., Lorrain, A., Sonke, J.E., Jaquemet, S., Schaal, G., Renedo, M., Besnard, L., Cherel, Y., Point, D., 2020b. Mercury Isotopes as Tracers of Ecology and Metabolism in Two Sympatric Shark Species. Environ. Pollut. 265, 114931 https://doi.org/10.1016/j.envpol.2020.114931.
Lee, C.-S., Lutcavage, M.E., Chandler, E., Madigan, D.J., Cerrato, R.M., Fisher, N.S., 2016. Declining Mercury Concentrations in Bluefin Tuna Reflect Reduced Emissions to the North Atlantic Ocean. Environ. Sci. Technol. 50 (23), 12825–12830. https://doi.org/10.1021/acs.est.6b04328.
Lee, K.A., Butcher, P.A., Harcourt, R.G., Patterson, T.A., Peddemors, V.M., Roughan, M., Harasti, D., Smoothey, A.F., Bradford, R.W., 2021. Oceanographic Conditions Associated with White Shark (Carcharodon carcharias) Habitat Use along Eastern Australia. Mar. Ecol. Prog. Ser. 659, 143–159. https://doi.org/10.3354/meps13572.
Lepak, R.F., Janssen, S.E., Yin, R., Krabbenhoft, D.P., Ogorek, J.M., DeWild, J.F., Tate, M.T., Holsen, T.M., Hurley, J.P., 2018. Factors Affecting Mercury Stable Isotopic Distribution in Piscivorous Fish of the Laurentian Great Lakes. Environ. Sci. Technol. 52 (5), 2768–2776. https://doi.org/10.1021/acs.est.7b06120.
Li, M., Juang, C.A., Ewald, J.D., Yin, R., Mikkelsen, B., Krabbenhoft, D.P., Balcom, P.H., Dassuncao, C., Sunderland, E.M., 2020. Selenium and Stable Mercury Isotopes Provide New Insights into Mercury Toxicokinetics in Pilot Whales. Sci. Total Environ. 710, 136325 https://doi.org/10.1016/j.scitotenv.2019.136325.
López-Berenguer, G., Peñalver, J., Martínez-López, E., 2020. A Critical Review about Neurotoxic Effects in Marine Mammals of Mercury and Other Trace Elements. Chemosphere 246, 125688. https://doi.org/10.1016/j.chemosphere.2019.125688.
Manceau, A., Bourdineaud, J.-P., Oliveira, R.B., Sarrazin, S.L.F., Krabbenhoft, D.P., Eagles-Smith, C.A., Ackerman, J.T., Stewart, A.R., Ward-Deitrich, C., del Castillo Busto, M.E., Goenaga-Infante, H., Wack, A., Retegan, M., Detlefs, B., Glatzel, P., Bustamante, P., Nagy, K.L., Poulin, B.A., 2021. Demethylation of Methylmercury in Bird, Fish, and Earthworm. Environ. Sci. Technol. 55 (3), 1527–1534. https://doi.org/10.1021/acs.est.0c04948.
Masbou, J., Point, D., Sonke, J.E., 2013. Application of a Selective Extraction Method for Methylmercury Compound Specific Stable Isotope Analysis (MeHg-CSIA) in Biological Materials. J. Anal. . Spectrom. 28 (10), 1620–1628. https://doi.org/10.1039/C3JA50185J.
Masbou, J., Sonke, J.E., Amouroux, D., Guillou, G., Becker, P.R., Point, D., 2018. Hg-Stable Isotope Variations in Marine Top Predators of the Western Arctic Ocean. ACS Earth Space Chem. https://doi.org/10.1021/acsearthspacechem.8b00017.
Matulik, A.G., Kerstetter, D.W., Hammerschlag, N., Divoll, T., Hammerschmidt, C.R., Evers, D.C., 2017. Bioaccumulation and Biomagnification of Mercury and Methylmercury in Four Sympatric Coastal Sharks in a Protected Subtropical Lagoon. Mar. Pollut. Bull. 116 (1), 357–364. https://doi.org/10.1016/j.marpolbul.2017.01.033.
May, C.; Meyer, L.; Whitmarsh, S.; Huveneers, C. 2019. Eyes on the Size: Accuracy of Visual Length Estimates of White Sharks, Carcharodon carcharias. *Royal Society Open Science 6* (5), 190456. https://doi.org/10.1098/rsos.190456.
McKinney, M.A., Dean, K., Hussey, N.E., Cliff, G., Wintner, S.P., Dudley, S.F.J., Zungu, M.P., Fisk, A.T., 2016. Global versus Local Causes and Health Implications of High Mercury Concentrations in Sharks from the East Coast of South Africa. Sci. Total Environ. 541, 176–183. https://doi.org/10.1016/j.scitotenv.2015.09.074.
Médieu, A., Point, D., Receveur, A., Gauthier, O., Allain, V., Pethybridge, H., Menkes, C.E., Gillikin, D.P., Revill, A.T., Somes, C.J., Collin, J., Lorrain, A., 2021. Stable Mercury Concentrations of Tropical Tuna in the South Western Pacific Ocean: An 18-Year Monitoring Study. Chemosphere 263, 128024. https://doi.org/10.1016/j.chemosphere.2020.128024.
Meng, M., Sun, R., Liu, H., Yu, B., Yin, Y., Hu, L., Chen, J., Shi, J., Jiang, G., 2020. Mercury Isotope Variations within the Marine Food Web of Chinese Bohai Sea: Implications for Mercury Sources and Biogeochemical Cycling. J. Hazard. Mater. 384, 121379 https://doi.org/10.1016/j.jhazmat.2019.121379.

Meyer, L., Fox, A., Huveneers, C., 2018. Simple Biopsy Modification to Collect Muscle Samples from Free-Swimming Sharks. Biol. Conserv. 228, 142–147. https://doi.org/10.1016/j.biocon.2018.10.024.

Meyer, L., Pethybridge, H., Beckmann, C., Bruce, B., Huveneers, C., 2019. The Impact of Wildlife Tourism on the Foraging Ecology and Nutritional Condition of an Apex Predator. Tour. Manag. 75, 206–215. https://doi.org/10.1016/j.tourman.2019.04.025.

Moro, S., Jona-Lasinio, G., Block, B., Micheli, F., Leo, G.D., Serena, F., Bottaro, M., Scacco, U., Ferretti, F., 2020. Abundance and Distribution of the White Shark in the Mediterranean Sea. Fish Fish 21 (2), 338–349. https://doi.org/10.1111/faf.12432.

Motta, L.C., Blum, J.D., Johnson, M.W., Umhau, B.P., Popp, B.N., Washburn, S.J., Drazen, J.C., Benitez-Nelson, C.R., Hannides, C.C.S., Close, H.G., Lamborg, C.H., 2019. Mercury Cycling in the North Pacific Subtropical Gyre as Revealed by Mercury Stable Isotope Ratios. Glob. Biogeochem. Cycles 33 (6), 777–794. https://doi.org/10.1029/2018GB006057.

Motta, L.C., Blum, J.D., Popp, B.N., Drazen, J.C., Close, H.G., 2020. Mercury Stable Isotopes in Flying Fish as a Monitor of Photochemical Degradation of Methylmercury in the Atlantic and Pacific Oceans. Mar. Chem. 223, 103790 https://doi.org/10.1016/j.marchem.2020.103790.

Myers, R.A., Worm, B., 2003. Rapid Worldwide Depletion of Predatory Fish Communities. Nature 423 (6937), 280–283. https://doi.org/10.1038/nature01610.

Nalluri, D., Baumann, Z., Abercrombie, D.L., Chapman, D.D., Hammerschmidt, C.R., Fisher, N.S., 2014. Methylmercury in Dried Shark Fins and Shark Fin Soup from American Restaurants. Sci. Total Environ. 496, 644–648. https://doi.org/10.1016/j.scitotenv.2014.04.107.

Obrist, D., Agnan, Y., Jiskra, M., Olson, C.L., Colegrove, D.P., Hueber, J., Moore, C.W., Sonke, J.E., Helmig, D., 2017. Tundra Uptake of Atmospheric Elemental Mercury Drives Arctic Mercury Pollution. Nature 547 (7662), 201–204. https://doi.org/10.1038/nature22997.

Ohkouchi, N., Chikaraishi, Y., Close, H.G., Fry, B., Larsen, T., Madigan, D.J., McCarthy, M.D., McMahon, K.W., Nagata, T., Naito, Y.I., Ogawa, N.O., Popp, B.N., Steffan, S., Takano, Y., Tayasu, I., Wyatt, A.S.J., Yamaguchi, Y.T., Yokoyama, Y., 2017. Advances in the Application of Amino Acid Nitrogen Isotopic Analysis in Ecological and Biogeochemical Studies. Org. Geochem. 113, 150–174. https://doi.org/10.1016/j.orggeochem.2017.07.009.

Pacoureau, N., Rigby, C.L., Kyne, P.M., Sherley, R.B., Winker, H., Carlson, J.K., Fordham, S.V., Barreto, R., Fernando, D., Francis, M.P., Jabado, R.W., Herman, K.B., Liu, K.-M., Marshall, A.D., Pollom, R.A., Romanov, E.V., Simpfendorfer, C.A., Yin, J. S., Kindsvater, H.K., Dulvy, N.K., 2021. Half a Century of Global Decline in Oceanic Sharks and Rays. Nature 589 (7843), 567–571. https://doi.org/10.1038/s41586-020-03173-9.

Perrot, V., Landing, W.M., Grubbs, R.D., Salters, V.J.M., 2019. Mercury Bioaccumulation in Tilefish from the Northeastern Gulf of Mexico 2 years after the Deepwater Horizon Oil Spill: Insights from Hg, C, N and S Stable Isotopes. Sci. Total Environ. 666, 828–838. https://doi.org/10.1016/j.scitotenv.2019.02.295.

Perrot, V.;, Masbou, J.; V., Pastukhov, M.; N., Epov, V.;, Point, D.;, Bérail, S.; R., Becker, P.; E., Sonke, J.;, Amouroux, D., 2016. Natural Hg Isotopic Composition of Different Hg Compounds in Mammal Tissues as a Proxy for in Vivo Breakdown of Toxic Methylmercury. Metallomics 8 (2), 170–178. https://doi.org/10.1039/C5MT00286A.

Peterson, S.H., Ackerman, J.T., Costa, D.P., 2015. Marine Foraging Ecology Influences Mercury Bioaccumulation in Deep-Diving Northern Elephant Seals. Proc. R. Soc. B: Biol. Sci. 282 (1810), 20150710 https://doi.org/10.1098/rspb.2015.0710.

Pethybridge, H., Cossa, D., Butler, E.C.V., 2010a. Mercury in 16 Demersal Sharks from Southeast Australia: Biotic and Abiotic Sources of Variation and Consumer Health Implications. Mar. Environ. Res. 69 (1), 18–26. https://doi.org/10.1016/j.marenvres.2009.07.006.

Pethybridge, H., Daley, R., Virtue, P., Butler, E.C.V., Cossa, D., Nichols, P.D., Pethybridge, H., Daley, R., Virtue, P., Butler, E.C.V., Cossa, D., Nichols, P.D., 2010b. Lipid and Mercury Profiles of 61 Mid-trophic Species Collected off South-eastern Australia. Mar. Freshw. Res. 61 (10), 1092–1108. https://doi.org/10.1071/MF09237.

Pimiento, C., Leprieur, F., Silvestro, D., Lefcheck, J.S., Albouy, C., Rasher, D.B., Davis, M., Svenning, J.-C., Griffin, J.N., 2020. Functional Diversity of Marine Megafauna in the Anthropocene. Sci. Adv. 6 (16), eaay7650. https://doi.org/10.1126/sciadv.aay7650.

Pinzone, M., Cransveld, A., Tessier, E., Bérail, S., Schnitzler, J., Das, K., Amouroux, D., 2021. Contamination Levels and Habitat Use Influence Hg Accumulation and Stable Isotope Ratios in the European Seabass Dicentrarchus labrax. Environ. Pollut. 281, 117008 https://doi.org/10.1016/j.envpol.2021.117008.

Poulin, B.A., Janssen, S.E., Rosera, T.J., Krabbenhoft, D.P., Eagles-Smith, C.A., Ackerman, J.T., Stewart, A.R., Kim, E., Baumann, Z., Kim, J.-H., Manceau, A., 2021. Isotope Fractionation from In Vivo Methylmercury Detoxification in Waterbirds. ACS Earth Space Chem. https://doi.org/10.1021/acsearthspacechem.1c00051.

Renedo, M., Amouroux, D., Pedrero, Z., Bustamante, P., Cherel, Y., 2018. Identification of Sources and Bioaccumulation Pathways of MeHg in Subantarctic Penguins: A Stable Isotopic Investigation. Sci. Rep. 8 (1), 8865. https://doi.org/10.1038/s41598-018-27079-9.

Renedo, M., Pedrero, Z., Amouroux, D., Cherel, Y., Bustamante, P., 2021. Mercury Isotopes of Key Tissues Document Mercury Metabolic Processes in Seabirds. Chemosphere 263, 127777. https://doi.org/10.1016/j.chemosphere.2020.127777.

Renedo, M., Point, D., Sonke, J.E., Lorrain, A., Demarcq, H., Graco, M., Grados, D., Gutiérrez, D., Médieu, A., Munaron, J.M., Pietri, A., Colas, F., Tremblay, Y., Roy, A., Bertrand, A., Bertrand, S.L., 2021. ENSO Climate Forcing of the Marine Mercury Cycle in the Peruvian Upwelling Zone Does Not Affect Methylmercury Levels of Marine Avian Top Predators. Environ. Sci. Technol. https://doi.org/10.1021/acs.est.1c03861.

Rodrigues, A.C.M.;, Gravato, C.;, Galvão, D.;, Silva, V.S.;, Soares, A.M.V.M.;, Gonçalves, J.M.S.;, Ellis, J.R.;, Vieira, R., 2021. Ecophysiological Effects of Mercury Bioaccumulation and Biochemical Stress in the Deep-Water Mesopredator Etmopterus spinax (Elasmobranchii; Etmopteridae). J. Hazard. Mater., 127245 https://doi.org/10.1016/j.jhazmat.2021.127245.

Sackett, D.K., Drazen, J.C., Popp, B.N., Choy, C.A., Blum, J.D., Johnson, M.W., 2017. Carbon, Nitrogen, and Mercury Isotope Evidence for the Biogeochemical History of Mercury in Hawaiian Marine Bottomfish. Environ. Sci. Technol. 51 (23), 13976–13984. https://doi.org/10.1021/acs.est.7b04893.

Schartup, A.T., Thackray, C.P., Qureshi, A., Dassuncao, C., Gillespie, K., Hanke, A., Sunderland, E.M., 2019. Climate Change and Overfishing Increase Neurotoxicant in Marine Predators. Nature 572 (7771), 648–650. https://doi.org/10.1038/s41586-019-1468-9.

Senn, D.B., Chesney, E.J., Blum, J.D., Bank, M.S., Maage, A., Shine, J.P., 2010. Stable Isotope (N, C, Hg) Study of Methylmercury Sources and Trophic Transfer in the Northern Gulf of Mexico. Environ. Sci. Technol. 44 (5), 1630–1637. https://doi.org/10.1021/es902361j.

Spaet, J.L.Y., Manica, A., Brand, C.P., Gallen, C., Butcher, P.A., 2020. Environmental Conditions Are Poor Predictors of Immature White Shark Carcharodon carcharias Occurrences on Coastal Beaches of Eastern Australia. Mar. Ecol. Prog. Ser. 653, 167–179. https://doi.org/10.3354/meps13488.

Spaet, J.L.Y.;, Patterson, T.A.;, Bradford, R.W.;, Butcher, P.A., 2020. Spatiotemporal Distribution Patterns of Immature Australasian White Sharks (Carcharodon carcharias). Sci. Rep. 10 (1), 10169. https://doi.org/10.1038/s41598-020-66876-z.

Sun, L., Chen, W., Yuan, D., Zhou, L., Lu, C., Zheng, Y., 2021. Distribution and Transformation of Mercury in Subtropical Wild-Caught Seafood from the Southern Taiwan Strait. Biol. Trace Elem. Res. https://doi.org/10.1007/s12011-021-02695-1.

Tate, R.D., Cullis, B.R., Smith, S.D.A., Kelaher, B.P., Brand, C.P., Gallen, C.R., Mandelman, J.W., Butcher, P.A., 2019. The Acute Physiological Status of White Sharks (Carcharodon carcharias) Exhibits Minimal Variation after Capture on SMART Drumlines. Conserv. Physiol. 7 (1), coz042. https://doi.org/10.1093/conphys/coz042.

Tate, R.D., Kelaher, B.P., Brand, C.P., Cullis, B.R., Gallen, C.R., Smith, S.D.A., Butcher, P. A., 2021. The Effectiveness of Shark-Management-Alert-in-Real-Time (SMART) Drumlines as a Tool for Catching White Sharks, *Carcharodon carcharias*, off Coastal New South Wales, Australia (fme). Fish. Manag Ecol. 12489. https://doi.org/10.1111/fme.12489.

Tsui, M.T.-K., Blum, J.D., Kwon, S.Y., 2020. Review of Stable Mercury Isotopes in Ecology and Biogeochemistry. Sci. Total Environ. 716, 135386 https://doi.org/10.1016/j.scitotenv.2019.135386.

Vo, A.-T.E., Bank, M.S., Shine, J.P., Edwards, S.V., 2011. Temporal Increase in Organic Mercury in an Endangered Pelagic Seabird Assessed by Century-Old Museum Specimens. PNAS 108 (18), 7466–7471. https://doi.org/10.1073/pnas.1013865108.

Wang, W.-X., Wong, R.S.K., 2003. Bioaccumulation Kinetics and Exposure Pathways of Inorganic Mercury and Methylmercury in a Marine Fish, the Sweetlips Plectorhinchus gibbosus. Mar. Ecol. Prog. Ser. 261, 257–268. https://doi.org/10.3354/meps261257.

Yurkowski, D.J., Richardson, E.S., Lunn, N.J., Muir, D.C.G., Johnson, A.C., Derocher, A. E., Ehrman, A.D., Houde, M., Young, B.G., Debets, C.D., Sciullo, L., Thiemann, G.W., Ferguson, S.H., 2020. Contrasting Temporal Patterns of Mercury, Niche Dynamics, and Body Fat Indices of Polar Bears and Ringed Seals in a Melting Icescape. Environ. Sci. Technol. 54 (5), 2780–2789. https://doi.org/10.1021/acs.est.9b06656.

Zheng, W., Foucher, D., Hintelmann, H., 2007. Mercury Isotope Fractionation during Volatilization of Hg(0) from Solution into the Gas Phase. J. Anal. At. Spectrom. 22 (9), 1097–1104. https://doi.org/10.1039/B705677J.